

Electrochemical Polymerization of Aniline and *N*-Alkylanilines

Akira Watanabe,\* Kunio Mori, Atsushi Iwabuchi, Yasunori Iwasaki, and Yoshiro Nakamura

Department of Applied Chemistry, Faculty of Engineering, Iwate University, Ueda, Morioka 020, Japan

Osamu Ito

Chemical Research Institute of Non-aqueous Solutions, Tohoku University, Katahira, Sendai 980, Japan. Received December 13, 1988;  
Revised Manuscript Received February 9, 1989

**ABSTRACT:** *N*-Alkylanilines were electrochemically oxidized in H<sub>2</sub>SO<sub>4</sub> aqueous solution. The electrochemical, spectroscopic, and electric properties of the oxidation products were investigated by comparing them with those of polyaniline. Although the film-forming ability on the electrode surface decreases with the bulkiness of the alkyl group, the solubility of the oxidation products increased with increasing the bulkiness of the alkyl group. The oxidation products of *N*-ethyl-, *N*-propyl-, and *N*-butylaniline are almost soluble in THF. From the GPC elution pattern showing the existence of high molecular weight components, formation of poly(*N*-alkylaniline)s was confirmed. The electric conductivities of these polymers were decreased by the bulkiness of the substituents. An increase in the conductivity accompanies the shift of the absorption bands in the near-IR region to the longer wavelength and the significant changes of ESR signals.

## Introduction

It has been known for a long time that the electrolysis of aniline gives stable oxidation products such as "aniline black", "emeraldine", and "nigrosine".<sup>1-5</sup> Since electric conductivity and electrochemical activity of these oxidation products were elucidated, considerable attention has been given to polyaniline,<sup>6-9</sup> which has been applied to various devices.<sup>10-14</sup>

The electrolysis of *N*-alkylaniline derivatives has been also investigated. The formation of low molecular weight products which are soluble in aqueous solution has been reported.<sup>15-18</sup> Recently, the formation of a filmlike product was reported for substituted anilines.<sup>19</sup> However, the characterization of the oxidized insoluble components has not been investigated by spectroscopic methods. It is expected that the introduction of alkyl groups on the polymer backbone induces some changes of the electronic state and the solubility.<sup>20,21</sup> In this paper, therefore, we prepared the polymers of *N*-alkylanilines by electrochemical oxidation and examined electric properties of the oxidation products on the basis of spectroscopic data. Different properties of the oxidation products among aniline and *N*-alkylanilines will provide useful information about the factors used to determine the various properties of polyaniline and derivatives.

## Experimental Section

**Materials.** *N*-Alkylanilines were electrochemically oxidized by the galvanostatic method in 1 M *N*-alkylaniline aqueous solutions containing 1 M H<sub>2</sub>SO<sub>4</sub> in the case of aniline, a 0.5 M aqueous solution containing 0.5 M H<sub>2</sub>SO<sub>4</sub> was used because of its low solubility. As *N*-alkylanilines, the methyl, ethyl, *n*-propyl, and *n*-butyl derivatives (Tokyo Kasei) were used. The surface of the Pt electrode was polished with 0.3- $\mu$ m Al<sub>2</sub>O<sub>3</sub> powder and then washed with deionized water, EtOH, and trichloroethylene.

**Measurements.** A potentiostat/galvanostat (Hokuto HA-201) and a function generator (Hokuto HB-103) were used for the measurements of cyclic voltammograms and the chemical oxidation of aniline and *N*-alkylanilines. Electrochemical potentials were recorded versus a saturated calomel electrode (SCE). GPC analyses were carried out by using Shodex columns A-802 and KF-803 (Showa Denko) with THF eluent. Monodispersed polystyrenes were used as standards in the GPC analysis. The optical spectra (in the UV, vis, near-IR, and IR regions) of the insoluble products were measured by the KBr pellet method. The 0.5 wt % sample was dispersed in KBr and compressed to under 600 kg/cm<sup>2</sup>. The IR and near-IR spectra were measured by a JEOL 100 type FT-IR spectrometer. The UV, vis, and near-IR

spectra were measured by a Jasco Ubest 30 type spectrometer. The ESR measurements were carried out by a Varian E-4 ESR spectrometer. The *g* value and spin density were determined using the signal of DPPH (1,1-diphenyl-2-picrylhydrazyl) free radical as the standard. The intensity of the double-integral ESR spectra for the 0.5 wt % sample concentration in KBr was compared with that of DPPH with the same concentration to determine the spin density. These ESR measurements were carried out under vacuum in order to avoid the influence of the oxygen adsorption. The conductivity of polymers was measured by the four-probe method preparing pellets of oxidation products (diameter of 13 mm with a pressure of 400 kg/cm<sup>2</sup>). The conductivity of polyaniline was measured for the pellet prepared after pulverizing the film. All these measurements were carried out at 22 °C.

## Results

**Electrochemical Oxidation of Aniline and *N*-Alkylanilines.** Cyclic voltammetry of *N*-alkylanilines showed oxidation peaks of *N*-alkylanilines at ca. 1.2 V versus SCE and redox peaks of oxidation products at ca. 0.5 V. They were irreversible and irreproducible because the oxidation products are soluble and easily eluted into the bulk solution from the electrode. The deposition of the film was hardly observed even by increasing the concentration of *N*-alkylanilines and H<sub>2</sub>SO<sub>4</sub> up to 1.0 M. For alkyl derivatives with a smaller alkyl group such as *N*-methylaniline, a slight amount of bluish green product remained on the electrode surface. On the other hand, for the electrolysis of unsubstituted aniline, stable polyaniline films were deposited on the electrode surface, showing reversible and reproducible cyclic voltammograms.<sup>6-9,13,14</sup>

In the early stage of the galvanostatic oxidation of *N*-alkylanilines, a large portion of the blue products was soluble in acidic aqueous solution as mentioned above. With increasing reaction time, however, a precipitate appeared in the solution. In order to collect enough oxidation products of *N*-alkylanilines, the electrolysis had to be performed in a concentrated solution, 1 M *N*-alkylaniline-1 M H<sub>2</sub>SO<sub>4</sub> aqueous solution. In the case of the electrolysis of aniline, a 0.5 M aniline-0.5 M H<sub>2</sub>SO<sub>4</sub> aqueous solution was used because of the relatively poor solubility.

Figure 1 shows the time dependence of potential versus SCE for galvanostatic oxidation of aniline and *N*-alkylanilines at 5 mA/cm<sup>2</sup>. During the galvanostatic oxidation of *N*-butyl- and *N*-propylaniline, the oxidation potential increased rapidly as shown in Figure 1, whereas the oxidation potentials of aniline, *N*-methylaniline, and *N*-ethylaniline are constant at ca. 0.7 V. Cyclic voltammetry

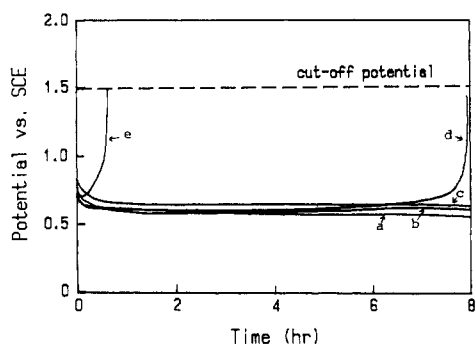


**Figure 1.** Change of potential with the reaction time for the galvanostatic oxidation of aniline in a 0.5 M aniline–0.5 M H<sub>2</sub>SO<sub>4</sub> aqueous solution and *N*-alkylanilines in a 1 M *N*-alkylaniline–1 M H<sub>2</sub>SO<sub>4</sub> aqueous solution at 5 mA/cm<sup>2</sup>. (a) Aniline, (b) *N*-methylaniline, (c) *N*-ethylaniline, (d) *N*-propylaniline, (e) *N*-butylaniline.

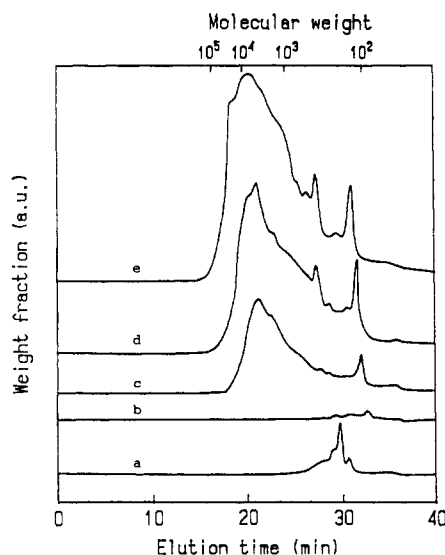


**Figure 2.** GPC elution patterns for electrolysis products of aniline and *N*-alkylanilines. Sample: 5 mg of oxidation product in 10 mL of THF. (a) Aniline, (b) *N*-methylaniline, (c) *N*-ethylaniline, (d) *N*-propylaniline, (e) *N*-butylaniline.

grams of *N*-alkylaniline showed anodic oxidation current of *N*-alkylanilines in the range between 0.6 and 1.5 V. Therefore, we set a cut-off potential of anodic oxidation at 1.5 V in order to minimize the degradation of products by further oxidation. Kobayashi et al. have reported that polyanilines degrade by excess oxidation.<sup>22</sup> The sudden increase of the potential during the oxidation of *N*-butyl- and *N*-propylaniline is attributable to the formation of passive deposit on the electrode.

The solubility of the oxidation products changed with the bulkiness of the alkyl group. Figure 2 shows GPC elution patterns using THF as an eluent. Sample solutions were prepared by dissolving 5 mg of the oxidation products in 10 mL of THF. The oxidation products of *N*-butylaniline were almost dissolved in THF. However, with decreasing bulkiness of the alkyl group, the insoluble residue increased. By the intensity of the elution peak in Figure 2, it is possible to compare the solubility. The oxidation products of *N*-methylaniline and aniline were almost insoluble in THF. Figure 2 gives information about the molecular weight of oxidation products. The highest molecular weights for elution peaks of the oxidation products of *N*-butyl, *N*-propyl, and *N*-ethylaniline are 20 000, 8000, and 4700, respectively. Therefore, they can be called poly(*N*-butylaniline), poly(*N*-propylaniline), and poly(*N*-ethylaniline). For insoluble polyaniline, we have

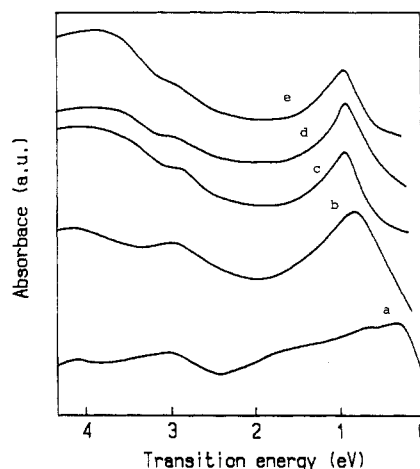


**Figure 3.** Absorption spectra of polyaniline and poly(*N*-alkylaniline)s. Sample: 0.5 mg/100 mg of KBr. (a) Aniline, (b) *N*-methylaniline, (c) *N*-ethylaniline, (d) *N*-propylaniline, (e) *N*-butylaniline.

**Table I**  
Electric Conductivity ( $\sigma$ ), Transition Energy of Broad-Band Peaks ( $A_{\max}$ ), and Doping Density for Polyaniline and Poly(*N*-alkylaniline)s

sample	$\sigma$ , S/cm	$A_{\max}$ , eV	doping density, SO <sub>4</sub> <sup>2-</sup> /monomer unit
polyaniline	$1.50 \times 10^1$	0.341	0.20
poly( <i>N</i> -methylaniline)	$2.09 \times 10^{-2}$	0.806	0.37
poly( <i>N</i> -ethylaniline)	$3.88 \times 10^{-6}$	0.893	0.15
poly( <i>N</i> -propylaniline)	$1.79 \times 10^{-6}$	0.899	0.13
poly( <i>N</i> -butylaniline)	$5.25 \times 10^{-8}$	0.969	0.13

reported that polyaniline has a molecular weight higher than 10 000, which became soluble after dedoping.<sup>23</sup> The insolubility of the oxidation products of *N*-methylaniline also suggests their high molecular weight.

**Characterization of Electropolymerized Products.** In Figure 3, the optical absorption spectra of polyaniline and poly(*N*-alkylaniline)s dispersed in a KBr disk measured throughout the region of UV, vis, near-IR, and IR are shown. The abscissa in Figure 3 is indicated by electronvolt units in order to compare the transition energies in wide region. The optical absorption spectra of polyaniline and poly(*N*-alkylaniline)s were characterized by the broad absorption band in the region of low transition energy (IR and near-IR region, 0.2–1.0 eV) and also by the absorption band at 2.95 eV (visible region near 420 nm). With an increase of the bulkiness of the alkyl group, the transition energy in the lower energy region increases as shown in Figure 3.

The electric conductivity measured with the four-probe method is summarized in Table I with the transition energy of the broad absorption band in the region of lower energy. The conductivity increases with lowering of the transition energy. The doping density of SO<sub>4</sub><sup>2-</sup> calculated from elemental analysis data is also shown in Table I. The elemental analysis showed the following values: C, 57.89; H, 4.48; N, 7.67; S, 5.18 for polyaniline; C, 54.74; H, 4.52; N, 8.67; S, 7.73 for poly(*N*-methylaniline); C, 68.55; H, 6.81; N, 9.83; S, 3.40 for poly(*N*-ethylaniline); C, 70.08; H, 7.00; N, 9.57; S, 2.70 for poly(*N*-propylaniline); C, 69.99; H, 7.37; N, 9.37; S, 3.21 for poly(*N*-butylaniline). These figures show that the degradation hardly occurs.

Figure 4 shows ESR spectra of polyaniline and poly(*N*-alkylaniline), which were measured using a powdered sample without dilution. The line width of ESR spectra

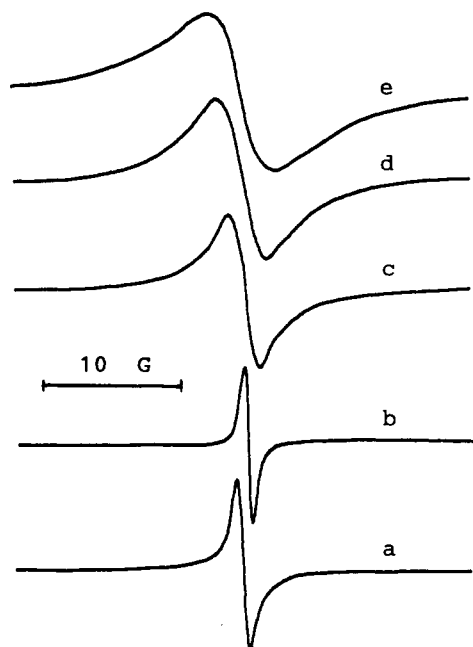


**Figure 4.** ESR spectra of polyaniline and poly(*N*-alkylaniline)s. (a) Aniline, (b) *N*-methylaniline, (c) *N*-ethylaniline, (d) *N*-propylaniline, (e) *N*-butylaniline.

**Table II**  
**ESR Parameters of Polyaniline and Poly(*N*-alkylaniline)s**

sample	<i>g</i>	spin density, unpaired electrons/g	$\Delta H$ , G
polyaniline	2.0035	$3.10 \times 10^{20}$	0.70
poly( <i>N</i> -methylaniline)	2.0034	$4.98 \times 10^{20}$	0.49
poly( <i>N</i> -ethylaniline)	2.0034	$8.15 \times 10^{20}$	0.98
poly( <i>N</i> -propylaniline)	2.0034	$3.85 \times 10^{20}$	3.30
poly( <i>N</i> -butylaniline)	2.0034	$2.96 \times 10^{20}$	4.85

increases with increasing the bulkiness on the alkyl group. The line width, ( $\Delta H$ ), *g* value, and spin density were summarized in Table II. The *g* values are similar to that of DPPH, 2.0036. The line widths of polyaniline and poly(*N*-methylaniline) are quite narrow even in comparison with that of DPPH, which is a typical example for spin-exchange narrowing ( $\Delta H = 1.3$  G). Figure 5 shows changes in the intensity of the ESR signal of polyaniline and poly(*N*-alkylaniline)s with microwave power. The change of the intensity with the microwave power is quite different among polyaniline and poly(*N*-alkylaniline)s. For example, poly(*N*-methylaniline) shows saturation at lower microwave power, whereas polyaniline does not show saturation within 50 mW of the microwave power.

## Discussion

In the early stage of the electrochemical oxidation of *N*-alkylaniline, a large portion of products is soluble. The further galvanostatic oxidation of *N*-alkylanilines gives precipitates. However, in the case of *N*-butyl and *N*-propylaniline, a sudden increase of the potential appeared in Figure 1. This must be caused by the precipitation of the oxidation products with low conductivity on the electrode. The bulkiness of the alkyl group decreases the electric conductivity of oxidation products as shown in Table I. The precipitates for all derivatives include stable radical cations as shown by the 2.95-eV (420-nm) peak in Figure 3, since the radical cations of aromatic amines show characteristic absorption at ca. 450 nm.<sup>24-27</sup> On the other hand, the soluble blue products at the early stage of the electrolysis were diamagnetic, suggesting the formation of diimine structures. The ESR signals shown in Figure 4

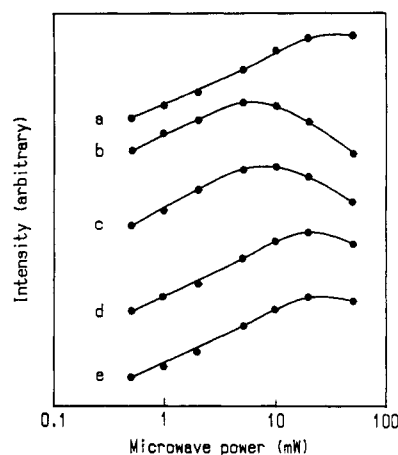


**Figure 5.** Change of the intensity of the ESR signals of polyaniline and poly(*N*-alkylaniline)s with microwave power. (a) Aniline, (b) *N*-methylaniline, (c) *N*-ethylaniline, (d) *N*-propylaniline, (e) *N*-butylaniline.

also support the existence of the radical cations in the precipitates. The *g* values of polyaniline and poly(*N*-alkylaniline)s are similar to that of DPPH, suggesting that their radical sites exist at the N atom.

The enhancement of the solubility of the conducting polymer by introducing substituents on the polymer backbone is a common technique.<sup>20,21</sup> In Figure 2, the solubility of the oxidation products increased with increasing the bulkiness of the alkyl group. In addition, the elution peaks of GPC suggest that the oxidation products of *N*-alkylaniline are not oligomers but polymers with high molecular weight components in the range from 20 000 to 4000. However, the conductivity decreased with increasing the bulkiness of the alkyl group as shown in Table I.

As one of factors determining the electric conductivity of the polymers, we have to consider the doping density of  $\text{SO}_4^{2-}$ . The conductivity of poly(*N*-alkylaniline)s increased with doping density calculated from elemental analysis data (Table I). However, the difference of about 3 orders magnitude for the conductivity between polyaniline and poly(*N*-methylaniline) cannot be explained only by the doping density because the electric conductivity of poly(*N*-methylaniline) with much dopant is still lower than that of polyaniline with less dopant.

The transition energy of the broad-band peak in the region of near-IR and IR shows correlation with the electric conductivity in Table I. The electric conductivity increases with lowering the transition energy. Polyaniline shows the lowest transition energy of 0.341 eV and the highest conductivity of  $1.50 \times 10^1$  S/cm. The broad-band peak is attributable to the transition from the valence band to an impurity level, which is induced by defect formation in the polymer. As a defect, the radical cation site which was observed by ESR measurements can be anticipated. The impurity level is located within the band gap of 4.00 eV, which is shown as an absorption peak in Figure 3. At a neutral state (fully dedoping state), a polyaniline film shows only peak at 4.00 eV without the broad-band peak. As an explanation for the energy diagram induced by defect formation, soliton,<sup>28-30</sup> polaron,<sup>9,31</sup> and bipolaron<sup>32</sup> models have been proposed for conductive polymers. The transition energy between the impurity level and the valence band edge can be interpreted as the activation energy for the carrier generation. For a homologous series of conductive polymers, polyaniline and poly(*N*-alkylaniline)s, the transition energy correlates with the conductivity as shown in Table I. When the transition energy decreases, the carrier generation which induces the electric conduc-

tivity increases. However, in the comparison with other series of conductive polymers, the relationship is not applicable because there is another factor, the mobility of the carrier, which relates closely to the chemical structure of the polymer backbone. For example, the transition energy of polyacetylene is 0.7 eV,<sup>33</sup> yet the conductivity is much higher than that for polyaniline with a transition energy of only 0.3 eV.

Another noticeable feature in Figure 3 is the band width in the low-energy region. Polyaniline with high conductivity has absorption in the wide region from 2.00 to 0.2 eV. The band width decreases with decreasing the conductivity, i.e., increasing the bulkiness of the alkyl group. In contrast to polyaniline, poly(*N*-butylaniline) shows a fairly narrow absorption near 1.00 eV. The width of the absorption is concerned with the interaction among electronic states; i.e., the strong interaction broadens the electronic level of the defect-induced states. The bulkiness of the alkyl group must decrease the interaction because the bulkiness in the polymer backbone hinders a planar structure of the conjugated electronic state.

ESR parameters also give valuable information about the correlation between the electric conductivity and the polymer structure. The line width of the ESR spectrum decreased with increasing the conductivity (Figure 4 and Table II). The spin-exchange interaction is one of the reasons for the narrowing of the ESR spectrum, which was caused by the high density of spin as known for DPPH. However, there is no correlation between the spin density and the line width,  $\Delta H$ , in Table II. Another reason for the narrowing is the spin diffusion in the polymer backbone. With respect to the electric conductive polyacetylene, the narrowing of the ESR signal is explained by the highly one-dimensional diffusive spin.<sup>34-37</sup> Recently, Glarum and Marshall suggested the three-dimensional spin diffusion in polyaniline based on the ESR line shapes.<sup>38</sup>

However, the explanation by the highly diffusive spin is not applicable to the case of polyaniline and poly(*N*-methylaniline) because the line width of poly(*N*-methylaniline) with the lower conductivity is narrower than that of polyaniline with the higher conductivity. Therefore, some additional reasons must be introduced. In Figure 5, the dependence of the intensity of the ESR signal on the microwave power shows a significant difference between polyaniline and poly(*N*-methylaniline). For poly(*N*-alkylaniline), the saturation point of the intensity of the ESR signal shifts to lower microwave power with decreasing the bulkiness of the alkyl group. However, with the change of the substituent from methyl group to hydrogen atom, discontinuity was observed; polyaniline shows no saturation point in the range under 50 mW. The saturation phenomena of the ESR signal intensity with the microwave power are closely related to the spin-lattice relaxation. It was reported that the spin-lattice relaxation time,  $T_1$ , for the polymers including polyacetylenes affords useful information about molecular motion near the radical center in polymers.<sup>39,40</sup> The saturation at low microwave power suggests long  $T_1$ , whereas that at high microwave power suggests short  $T_1$ .<sup>41,42</sup> It is expected that macromolecules with rigid structure show shorter  $T_1$  than those with flexible structure.<sup>41-43</sup> On the basis of above concept, polyaniline has a shorter  $T_1$  and rigid structure compared to poly(*N*-methylaniline), which has a longer  $T_1$  and flexible structure. The flexibility of poly(*N*-methylaniline) is due to the existence of a methyl group in the polymer backbone, whereas polyaniline has a rather planar structure and conjugated electronic state. The difference in polymer structures causes the significant difference of the

electric conductivity between polyaniline and poly(*N*-methylaniline).

The saturation point of the ESR signal of poly(*N*-alkylaniline)s shifts toward to higher microwave power with increasing the bulkiness of the alkyl group as shown in Figure 5. As an interpretation, one can consider that the molecular motion near the radical center decreases with increasing the bulkiness of alkyl group in the homologous series of poly(*N*-alkylaniline)s.

## Conclusion

By GPC analysis, it was suggested that electrochemical oxidation products of *N*-alkylanilines have high molecular weight components; thus, they are referred to as poly(*N*-alkylaniline). The conductivity decreased with increasing the bulkiness of the alkyl group, which are closely correlated with the spectroscopic data. Especially, the transition energy of the broad absorption peak in the near-IR and IR regions showed a correlation with the conductivity. When the transition energy, which corresponds to the activation energy for carrier generation, was decreased, the conductivity increased. The line width of the ESR spectrum also showed a correlation with the conductivity. When the line width decreased, the conductivity increased. The saturation phenomena of the intensity of the ESR signals with the microwave power suggested the significant difference of the spin-lattice relaxation caused by the difference in the polymer structure, which can explain the difference in the conductivity between polyaniline and poly(*N*-methylaniline) having similar line widths. Polyaniline has a more rigid structure than poly(*N*-methylaniline) because of the conjugated planar structure.

**Acknowledgment.** We thank Dr. Thomas Jando for helpful discussions. We also gratefully acknowledge the comments made by the reviewers of this manuscript.

**Registry No.** Polyaniline, 25233-30-1; poly(*N*-methylaniline), 27082-18-4; poly(*N*-ethylaniline), 88374-64-5; poly(*N*-propylaniline), 120743-26-2; poly(*N*-butylaniline), 120743-27-3.

## References and Notes

- Mohilner, D. M.; Adams, R. N.; Argersinger, W. J., Jr. *J. Am. Chem. Soc.* **1962**, *84*, 3618.
- Mizoguchi, T.; Adams, N. R. *J. Am. Chem. Soc.* **1962**, *84*, 2058.
- Green, A. G.; Woodhead, A. E. *J. Chem. Soc.* **1910**, 2388.
- Surville, R.; Josefowicz, M.; Yu, L. T.; Perichon, J.; Buvet, C. R. *Electrochim. Acta* **1968**, *13*, 1451.
- Cristofini, F.; Josefowicz, M.; Yu, L. T.; Buvet, C. R. *Acad. Sci. Paris, Ser. C* **1969**, *268*, 1346.
- Diaz, A. F.; Logan, J. A. *J. Electroanal. Chem.* **1980**, *111*, 111.
- MacDiarmid, A. G.; Chiang, J. C.; Halpern, M.; Huang, W. S.; Mu, S. L.; Somasiri, N. L. D.; Wu, W.; Yaniger, S. I. *Mol. Cryst. Liq. Cryst.* **1985**, *121*, 173.
- Huang, W. S.; Humphrey, B. D.; MacDiarmid, A. G. *J. Chem. Soc., Faraday Trans. 1* **1986**, *82*, 2385.
- Genies, E. M.; Lapkowski, M. *J. Electroanal. Chem.* **1987**, *220*, 67.
- Noufi, R.; Nozik, A. J.; White, J.; Warren, L. *J. Electrochem. Soc.* **1982**, *129*, 2261.
- Inganas, O.; Lundstron, I. *J. Electrochem. Soc.* **1984**, *131*, 1129.
- Oyama, N.; Ohsaka, T.; Shimizu, T. *Anal. Chem.* **1985**, *57*, 1526.
- Kobayashi, T.; Yoneyama, H.; Tamura, H. *J. Electroanal. Chem.* **1984**, *161*, 419.
- Watanabe, A.; Mori, K.; Iwasaki, Y.; Nakamura, Y.; Niizuma, S. *Macromolecules* **1987**, *20*, 1793.
- Hand, R. L.; Nelson, R. F. *J. Am. Chem. Soc.* **1974**, *93*, 850.
- Cauquis, J.; Cognard, J.; Serve, D. *Tetrahedron Lett.* **1971**, 4645.
- Hand, R.; Nelson, R. F. *J. Electrochem. Soc.* **1970**, *117*, 1353.
- Neubert, G.; Prater, K. B. *J. Electrochem. Soc.* **1974**, *121*, 745.
- Oyama, N.; Ohsaka, T. *Synth. Met.* **1987**, *18*, 375.
- Sato, M. A.; Tanaka, S.; Kaeriyama, K. *J. Chem. Soc., Chem. Commun.* **1986**, 1346.
- Hotta, S.; Rughooputh, S. D. D. V.; Heeger, A. J.; Wudl, F. *Macromolecules* **1987**, *20*, 212.

- (22) Kobayashi, T.; Yoneyama, H.; Tamura, H. *J. Electroanal. Chem.* **1984**, *177*, 293.  
 (23) Watanabe, A.; Mori, K.; Iwasaki, Y.; Nakamura, Y. *J. Chem. Soc., Chem. Commun.* **1987**, 3.  
 (24) Hakusui, A.; Matsunaga, Y.; Umehara, K. *Bull. Chem. Soc. Jpn.* **1970**, *43*, 709.  
 (25) Alkaitis, S. A.; Ratzel, M. *J. Am. Chem. Soc.* **1976**, *98*, 3549.  
 (26) Michaelis, L.; Schubert, M. P.; Gramick, S. *J. Am. Chem. Soc.* **1939**, *61*, 1981.  
 (27) Mcmanus, P. M.; Yang, S. C.; Cushman, R. *J. Chem. Soc., Chem. Commun.* **1985**, 1556.  
 (28) Su, W. P.; Schrieffer, J. R.; Heeger, A. J. *Phys. Rev. Lett.* **1979**, *42*, 1698.  
 (29) Rice, M. J. *Phys. Lett.* **1979**, *71A*, 152.  
 (30) Takayama, H.; Lin-Liu, Y. R.; Maki, K. *Phys. Rev. B* **1980**, *21*, 2388.  
 (31) Su, W. P.; Schrieffer, J. R. *Proc. Natl. Acad. Sci. U.S.A.* **1980**, *77*, 5626.  
 (32) Brédas, J. L.; Chance, R. R.; Silbey, R. *Mol. Cryst. Liq. Cryst.* **1981**, *77*, 319.  
 (33) Feldblum, A.; Kaufman, J. H.; Etemad, S.; Heeger, A. J.; Chung, T.-C.; MacDiarmid, A. G. *Phys. Rev. B* **1982**, *26*, 1815.  
 (34) Nechtschein, M.; Devreux, F.; Genoud, F.; Guglielmi, M.; Holczer, K. *Phys. Rev. B* **1983**, *27*, 61.  
 (35) Kinoshita, M.; Tokumoto, M. *J. Phys. Soc. Jpn.* **1981**, *50*, 2779.  
 (36) Kinoshita, N.; Tokumoto, M.; Shirakawa, H. *Mol. Cryst. Liq. Cryst.* **1982**, *83*, 67.  
 (37) Thomann, H.; Baker, G. L. *J. Am. Chem. Soc.* **1987**, *109*, 1569.  
 (38) Glarum, S. H.; Marshall, J. H. *J. Electrochem. Soc.* **1987**, *134*, 2160.  
 (39) Bullock, A. T.; Sutcliffe, L. H. *Trans. Faraday Soc.* **1964**, *60*, 2112.  
 (40) Chien, J. C. W.; Schen, M. A. *Macromolecules* **1986**, *19*, 1042.  
 (41) Ito, O.; Seki, H.; Iino, M. *Bull. Chem. Soc. Jpn.* **1987**, *60*, 2967.  
 (42) Seki, H.; Ito, O.; Iino, M. *Energy Fuels* **1988**, *2*, 321.  
 (43) Duber, S.; Wieckowski, A. B. *Fuel* **1982**, *61*, 433.

## New AB Polyesters and a Polymethacrylate Containing Dipolar *p*-Phenyleneazo Groups

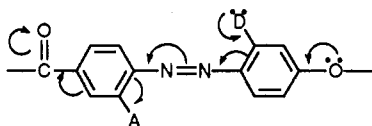
H. K. Hall, Jr.,<sup>\*,†</sup> Thauming Kuo,<sup>†</sup> and T. M. Leslie<sup>†</sup>

C. S. Marvel Laboratories, Department of Chemistry, University of Arizona, Tucson, Arizona 85721. Received December 13, 1988; Revised Manuscript Received February 28, 1989

**ABSTRACT:** The AB monomers 4-[(4-hydroxy-2-methoxyphenyl)azo]benzoic acid (1), 4-[[4-[(4-hydroxy-2-methoxyphenyl)azo]-2-methoxyphenyl]azo]benzoic acid (2), and 4-[(4-hydroxy-2-methoxyphenyl)azo]-3-nitrobenzoic acid (3) containing dipolar *p*-phenyleneazo groups were synthesized and subsequently polymerized. The monomers were polymerized by recently developed direct polycondensation techniques. The polyester synthesized from 1 forms a red, transparent film. Monomer 2 did not polymerize, while 3 gave a powdered polymer. A comblike polymethacrylate 9 containing dipolar *p*-phenyleneazo groups in the side chains was also prepared by the free radical polymerization of 1-[3-methoxy-4-[(*p*-nitrophenyl)azo]phenoxy]hexyl methacrylate (8). Polymer 9 showed a  $T_g$  at 88 °C followed by decomposition at 255 °C; liquid-crystalline behavior was observed in this temperature range. All the polymers were found to have little or no absorption at the wavelengths of telecommunication interest. They may be useful as nonlinear optical materials.

### Introduction

Polymers that possess high nonlinear optical activities have seen a recent growth in interest.<sup>1,2</sup> We have recently synthesized AB polyesters that contain highly dipolar quinodimethane units<sup>3</sup> or *p*-oxy- $\alpha$ -cyanocinnamate units<sup>4</sup> in the polymer main chain. These dipolar polyesters have been shown to possess a high nonlinear optical effect.<sup>5</sup> We have also previously synthesized polyesters containing multiple *p*-phenyleneazo groups, which have strongly delocalized  $\pi$  electrons.<sup>6</sup> The introduction of donor and acceptor substituents in a push-pull arrangement to these polymers through the diphenylazo group as shown below would make them highly attractive as polymeric nonlinear optical substrates.



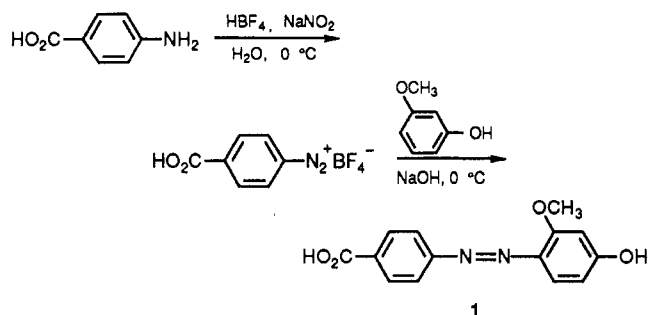
Similarly, these dipolar units shown above in the main chain can also be incorporated into the side chains of comblike polymethacrylates. Methacrylate or acrylate polymers containing dipolar azo groups in the side chains have recently been demonstrated to have a large third-order<sup>7</sup> or second-order<sup>8</sup> nonlinear optical effect.

### Results and Discussion

We have now synthesized two types of polymers containing dipolar *p*-phenyleneazo groups.

**Polyesters Containing Dipolar *p*-Phenyleneazo Units in the Main Chain.** AB monomers containing methoxy or nitro substituents on the *p*-phenyleneazo groups were prepared by diazotization and coupling. These monomers were polymerized by recent direct polycondensation techniques.

**Synthesis of the Monomers.** Monomer 1, 4-[(4-hydroxy-2-methoxyphenyl)azo]benzoic acid, was prepared by diazotization of *p*-aminobenzoic acid, followed by coupling with *m*-methoxyphenol.



Monomer 2, 4-[[4-(4-hydroxy-2-methoxyphenyl)-2-methoxyphenyl]azo]benzoic acid, containing two azo units was also synthesized by diazotization and coupling as shown in the following reaction sequence. The sequence

<sup>\*</sup> C.S. Marvel Laboratories.

<sup>†</sup> Hoechst-Celanese Co., 86 Morris Ave., Summit, NJ 07901.